

**UNCLASSIFIED**

---

---

**AD 295 750**

---

*Reproduced  
by the*

**ARMED SERVICES TECHNICAL INFORMATION AGENCY  
ARLINGTON HALL STATION  
ARLINGTON 12, VIRGINIA**



---

---

**UNCLASSIFIED**

**NOTICE:** When government or other drawings, specifications or other data are used for any purpose other than in connection with a definitely related government procurement operation, the U. S. Government thereby incurs no responsibility, nor any obligation whatsoever; and the fact that the Government may have formulated, furnished, or in any way supplied the said drawings, specifications, or other data is not to be regarded by implication or otherwise as in any manner licensing the holder or any other person or corporation, or conveying any rights or permission to manufacture, use or sell any patented invention that may in any way be related thereto.

ARPA Order No. 22-62

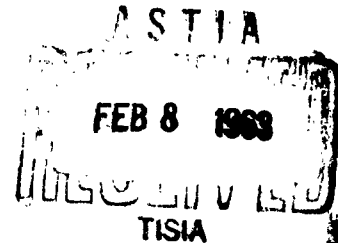
TG 331-15  
Copy No. 14

CATALOGED BY ASTIA  
AS AD No. 295750

**295 750**

**TASK R**  
**Quarterly Progress Report No. 15**  
**for the period**  
**1 Oct. - 31 Dec. 1962**

**TASK R IS A PROGRAM OF RESEARCH IN PHYSICO-CHEMICAL AND FLUID DYNAMIC PHENOMENA BASIC TO THE UNDERSTANDING OF HIGH-TEMPERATURE, HIGH-SPEED GAS FLOW. IT IS SUPPORTED BY THE ADVANCED RESEARCH PROJECTS AGENCY THROUGH CONTRACT NOW 62-0604-c WITH THE BUREAU OF NAVAL WEAPONS, DEPARTMENT OF THE NAVY.**



**THE JOHNS HOPKINS UNIVERSITY**  
**APPLIED PHYSICS LABORATORY**  
8621 GEORGIA AVENUE SILVER SPRING, MARYLAND

**NO OTS**

ARPA Order No. 22-62

TG 331-15

**TASK R**  
**Quarterly Progress Report No. 15**  
**for the period**  
**1 Oct. - 31 Dec. 1962**

**THE JOHNS HOPKINS UNIVERSITY**  
**APPLIED PHYSICS LABORATORY**  
8621 GEORGIA AVENUE                      SILVER SPRING, MARYLAND

## GENERAL OBJECTIVES OF TASK R

It seems likely that long-range development of improved propulsion systems will rely more and more upon a sound understanding and quantitative knowledge of the underlying physical and chemical phenomena involved. Many of these phenomena, and the practical problems arising in connection with them, have to do with the high temperatures characteristic of most advanced propulsion systems. Prediction of performance, the problems encountered with materials, heat transfer and cooling techniques - all these become more difficult and sophisticated with the trend to higher temperature operation, and will ultimately require a more fundamentally based understanding than is characteristic of the usual expensive "cut-and-try" or "quick-fix" test procedures.

Research performed under Task R at the Applied Physics Laboratory is intended to provide some of this basic knowledge in appropriate areas. The general emphasis is on the physico-chemical and fluid dynamic behavior of high temperature, high speed gas flows such as occur in most advanced propulsion systems.

A. A. Westenberg  
Program Coordinator

## SUMMARY

	<u>Page</u>
I. Dissociated Gas Studies	1
<p>Some preliminary trials using electron spin resonance to measure gas phase free radicals and atoms in a simple flow system are described. Sample spectra for <math>O_2</math>, O, and NO are presented. A comparison of the absolute concentration of O atoms measured by the ESR technique and by gas phase titration with <math>NO_2</math> is being attempted.</p>	
II. Thermal Conductivity of Gases	6
<p>Discrepancies between theory and experiment for the thermal conductivity of the <math>O_2 - H_2O</math> system as function of composition and temperature are discussed. It is shown that taking account in a semi-quantitative way of the resonant interchange of rotational energy for <math>H_2O</math> according to a recently developed theory helps to reduce the discrepancy.</p>	
III. Rocket Nozzle Fluid Dynamics	11
<p>Results to date with the fast scanning infrared spectrometer for determining the composition of rocket exhaust gases in situ are reviewed. It appears that the present technique for flushing the windows of the viewing ports with <math>N_2</math> needs improvement.</p>	
IV. Molecular Beam Chemical Kinetic Studies	16
<p>A proposal for a new technique of creating high intensity aerodynamic beams is described. This makes use of a porous wall nozzle which should reduce the pumping requirements. Some of the ideas involved in using beams for kinetic research are discussed.</p>	

## I. DISSOCIATED GAS STUDIES

(N. de Haas and A. A. Westenberg)

### Objective

Several aspects of the high temperature gas flow associated with most propulsion systems have to do with the behavior of dissociated gases containing various labile atoms and radicals. Heat transfer and mixing processes often involve the diffusion of such species and their reactions in gas boundary layers and at surfaces. Because of their high reactivity, reliable basic data on the transport and kinetic properties of atoms and radicals are difficult to obtain. The difficulties lie both in establishing a well-defined experimental system appropriate to the measurement to be carried out and in detecting and measuring the labile species themselves.

The present program represents an effort, first of all, to utilize the flow tube technique to study the diffusion and chemical kinetics of discharge-generated atoms and radicals under well-defined conditions. The detection system to be employed is that of electron spin resonance (ESR), since the unpaired electron(s) possessed by all free radicals makes this technique the most widely applicable of any presently available. Thus the objective of this research is to acquire the necessary know-how in ESR as a quantitative detector of atoms and radicals, and to use it in appropriate diffusion and kinetic studies of such species.

### The ESR System

A Varian V-4502 ESR spectrometer system is available for this work. Components of this system include a 9-inch magnet with a three-inch gap, a 100-kc field modulation unit and a multi-purpose

rectangular cavity operating in the TE-012 mode. Fields up to 9600 gauss are readily available with the magnet. Field measurements for the location and identification of lines are made with the aid of a proton resonance gaussmeter (Alpha AL67).

#### Flow System

For the purpose of checking out and learning to use the spectrometer, as well as to carry out preliminary O-atom concentration determinations, the flow system shown in Figure I-1 was constructed. An 8-mm i.d. quartz reaction tube passes through the resonant cavity located centrally in the magnet gap. A regulated and metered flow of O<sub>2</sub> passes through the tube. A portion of the O<sub>2</sub> is dissociated by a microwave discharge at the point where the tube passes through a slotted cavity resonator (Ref. 1). The mixture of O and O<sub>2</sub> passes through the ESR cavity, a needle valve, and then is exhausted by a vacuum pump. This needle valve is used to vary the pressure in the system for a given mass flow. An inlet to introduce other gases at a known small rate into the reaction tube just upstream of the ESR cavity is provided. The gaussmeter probe (not shown in Fig. I-1) is located alongside the ESR cavity.

#### ESR Spectra

Figures I-2 and I-3 show ESR spectra for the O-atom and for NO, respectively. These were obtained to show the capabilities of the spectrometer system and to serve as an introduction to tests that would involve these species. They compare well with the spectra given in Refs. 2 (O-atom) and 3 (NO).

The resolved O-atom spectrum consists of six lines centered at 4422 gauss for the cavity resonant frequency of 9285 mc: four <sup>3</sup>P<sub>2</sub> transitions and two satellite lines (<sup>3</sup>P<sub>1</sub> transitions). The NO spectrum is centered at approximately 8600 gauss and consists of nine lines of

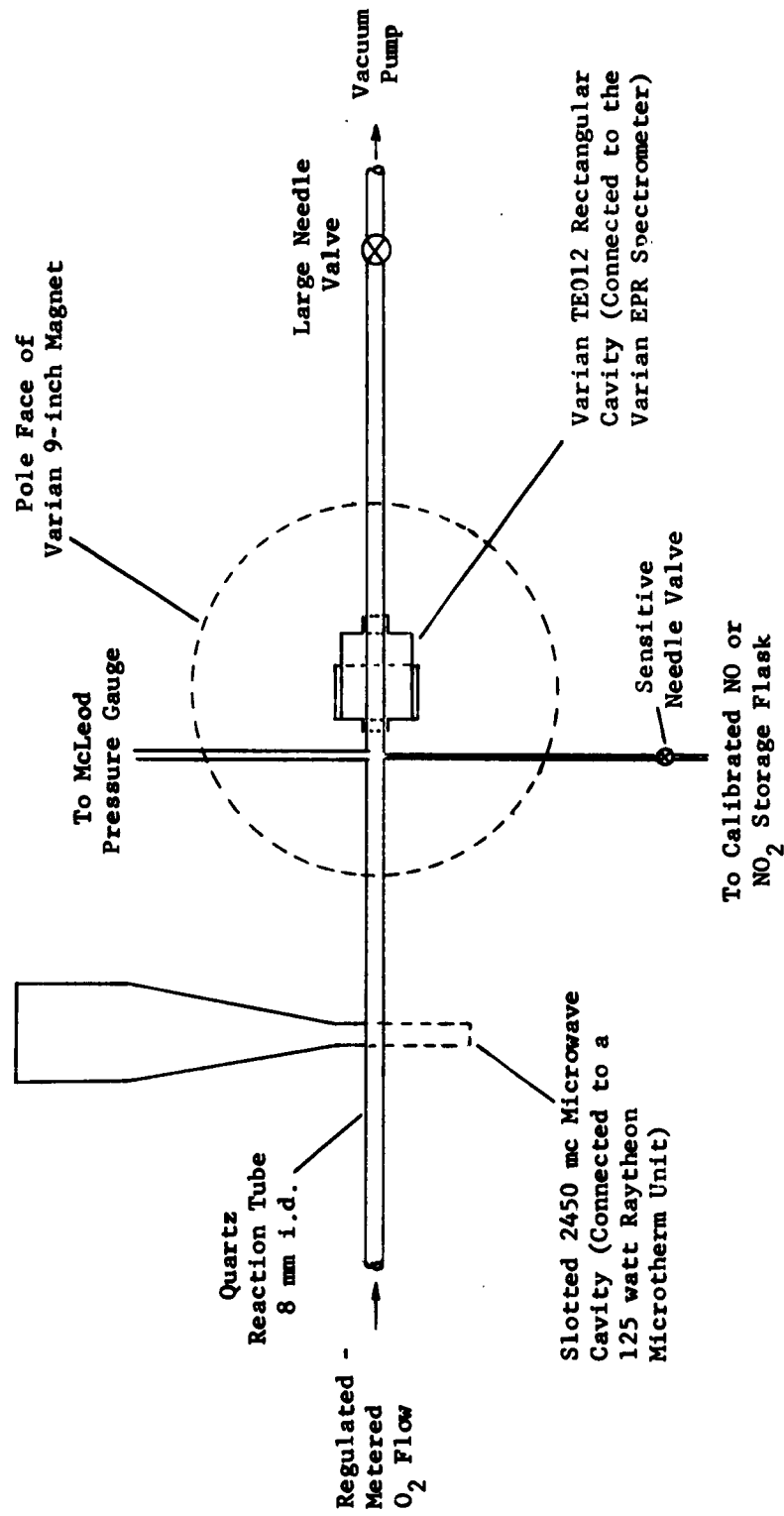


Fig. I-1. Flow System for O-Atom Concentration Measurements.

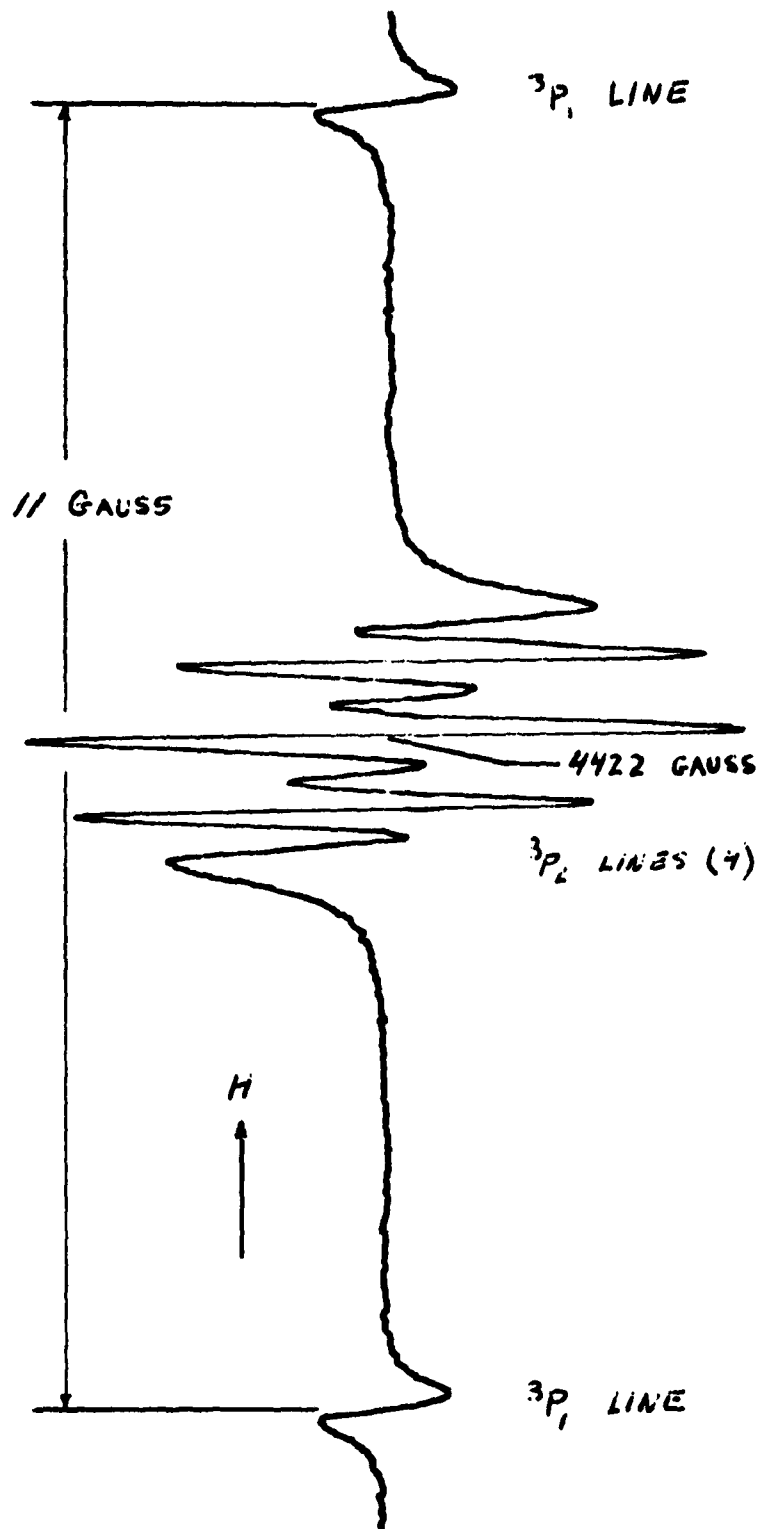


Fig. I-2 ATOMIC OXYGEN ELECTRON SPIN RESONANCE SPECTRUM;  
 FIRST DERIVATIVE OF ABSORPTION  
 VS MAGNETIC FIELD STRENGTH

Pressure = 0.051 mm Hg (O + O<sub>2</sub>). Spectrometer:  
 attenuation = 14 db; modulation = .16 gauss  
 100 kc; signal = 160; cavity resonance frequency =  
 9285 mc; and sweep time = 10 min.

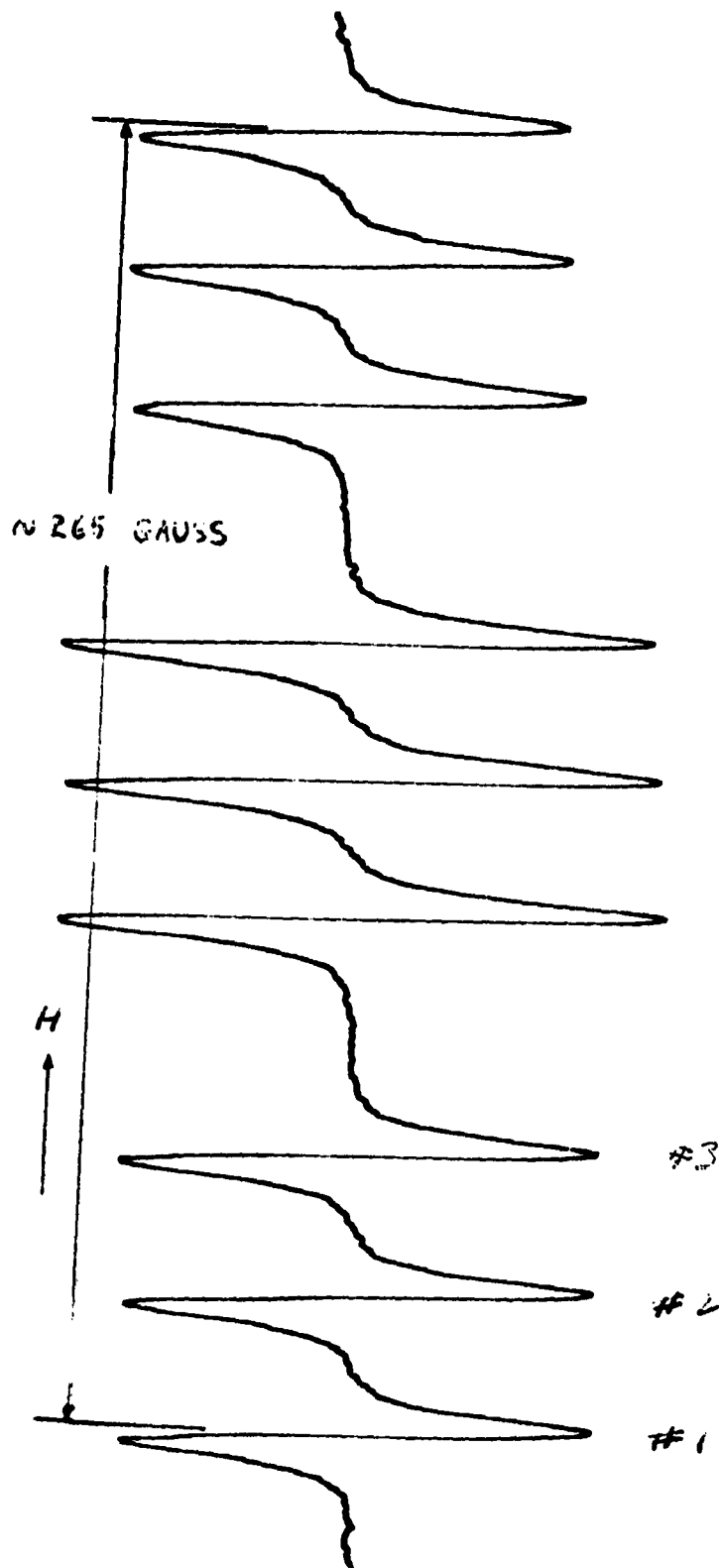


Fig. I-3 NITRIC OXIDE ELECTRON SPIN RESONANCE SPECTRUM (transition in  $J = 3/2$  level of the  $2_{3/2}$  state): FIRST DERIVATIVE OF ABSORPTION VS MAGNETIC FIELD STRENGTH

Spectrum centered at approximately 8600 gauss.  
 Pressure = 0.6 mm Hg (NO). Spectrometer:  
 attenuation = 7 db; modulation = 8 gauss  
 100 kc; signal = 320; cavity resonance  
 frequency = 9285 mc; and sweep time = 10 min.

transitions in the  $J = 3/2$  level of the  $^2\Pi_{3/2}$  state. These lines were obtained with only NO flowing through the reaction tube; the presence of  $O_2$  would have obscured all of the NO lines except the two at the lowest field values.

The conditions of flow and spectrometer settings are given in the captions to the figures. A comparison of these conditions shows that the magnitude of a single NO line is a factor of 1000-3000 lower than the 4 central lines of the O-atom spectrum (assuming 1-2% O-atoms in  $O_2$  and neglecting modulation differences for the two spectra). A large difference in magnetic field sweep rate is also evident in these spectra (the chart speeds were the same). These comparisons serve to show in a cursory way the versatility of the ESR spectrometer system.

#### O-Atom Concentration Measurements

In a preliminary way, two methods have been tried to date to determine the O-atom absolute concentration. These are (1) the ESR method of Krongelb and Strandberg (Ref. 2) who used an  $O_2$  line for calibration, and (2) the  $NO_2$  gas phase titration method used by Kaufman (Ref. 4).

The first method requires a comparison of the O-atom lines (six) with a known  $O_2$  line and a known concentration of  $O_2$ . The  $O_2$  line selected by Krongelb and Strandberg was the  $K = 5$ ,  $J = 4-6$ ,  $M = 1-2$  line for which they obtained the expression for relative concentrations,

$$\frac{N_O}{N_{O_2}} = 1.05 \times 10^{-3} \frac{\int_0^{\infty} \chi''_{O} dH}{\int_0^{\infty} \chi''_{O_2} dH}, \quad (1)$$

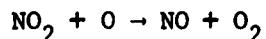
or

$$\frac{N_{O}}{N_{O_2}} = 1.05 \times 10^{-3} \frac{\int_0^{\infty} (H - H')_O (d\chi''_O/dH) dH}{\int_0^{\infty} (H - H')_{O_2} (d\chi''_{O_2}/dH) dH} \quad (2)$$

where  $H'$  is the resonant field strength and  $\chi''$  is the imaginary part of the spin susceptibility. The second expression is most convenient for use since the spectrometer output is proportional to  $d\chi''/dH$ .

Figure I-4 shows this  $O_2$  line and the O-lines\* in comparison. All of the conditions are the same for the two spectra except the magnetic field strength and the signal level (gain). Since the magnetic field sweep conditions are the same (although the absolute fields differ) Eq. 2 may be used without knowing the absolute field shape (i.e.  $H - H'$ ) of each line. Only a factor arising from different signal levels must be included. The application of Eq. 2 to the lines of Figure I-4 gave an atom concentration of 0.88%.

The  $NO_2$  titration method of O-atom concentration determination requires a known and controllable rate of  $NO_2$  injection into the  $O + O_2$  system and a means to know when the atom concentration is brought to zero by the very fast reaction



This is usually done by observing the extinction of the air afterglow (due to  $NO + O$  reaction). However, it was found that the ESR spectrometer provided a sensitive means to determine the point of extinction (disappearance of the O-line).

---

\* The O-lines shown in Figure I-4 differ from those in Figure I-2 partly because of a higher modulation in Figure I-4, but primarily because of pressure broadening.

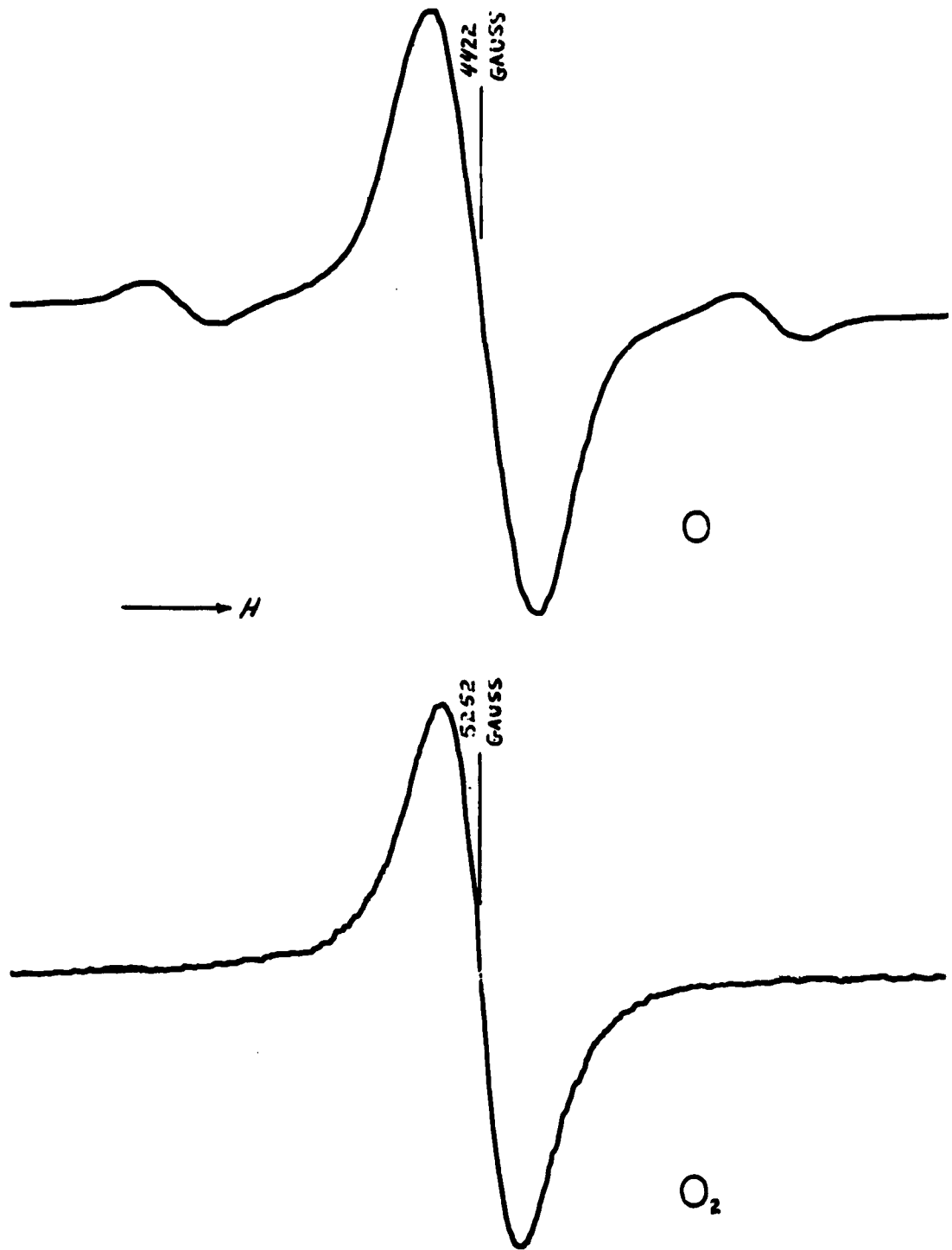


Fig. I-4 ATOMIC OXYGEN ESR LINES ( $^3P_1$  and  $^3P_2$  transitions) AND MOLECULAR OXYGEN LINE ( $K = 5$ ,  $J = 4 \rightarrow 6$ ,  $M = 1 \rightarrow 2$ ) IN COMPARISON FOR DETERMINATION OF RELATIVE CONCENTRATIONS OF ATOMS AND MOLECULES: FIRST DERIVATIVE OF ABSORPTION VS MAGNETIC FIELD STRENGTH

Flow Conditions: pressure = 0.53 mm Hg ( $O + O_2$ ) and velocity = 360 cm/sec. Spectrometer: attenuation = 14 db; modulation = 1.6 gauss 100 kc; signal = 25 (O), 250 ( $O_2$ ); cavity resonance frequency = 9285 mc; and sweep time = 10 min.

A comparison of these two methods to date show 50-100% higher measured concentration by the NO<sub>2</sub> titration than with the ESR. Work is now in progress to determine the reason(s) for this discrepancy.

References

- 1) H. P. Broida and M. W. Chapman, Anal. Chem. 30, 2049 (1958).
- 2) S. Krongelb and M. W. P. Strandberg, J. Chem. Phys. 31, 1196 (1959).
- 3) R. Beringer and J. G. Castle, Jr., Phys. Rev. 78, 581 (1950).
- 4) F. Kaufman, Proc. Roy. Soc. A247, 123 (1958).

## II. THERMAL CONDUCTIVITY OF GASES

(N. de Haas and A. A. Westenberg)

### Objective

The analysis of the problem of convective heat transfer both in the laminar and turbulent flow regimes requires that the properties of the gases involved be quantitatively understood. The coefficient of thermal conductivity is one such property. Measurement of this property has been the subject of considerable research over the years, but as far as reaction motor applications are concerned, the primary shortcomings of conventional past and present research in this area are: (a) The great difficulty in employing the usual apparatus (static hot wire cells) at temperatures more than a few hundred degrees above room temperature, and (b) the lack of data on species and mixtures characteristic of advanced propellant gases. Other shortcomings could be listed.

Recently, a new technique for measuring gas thermal conductivity has been developed in this Laboratory which represents a radical change in approach to the problem. A line source of heat (approximated by an electrically heated fine wire) is provided in a uniform, steady, laminar flow of the gas under study. Differential thermocouple measurement of the thermal wake downstream of this line source, together with a measurement of the gas velocity, allows the thermal conductivity to be determined. The method is simple, has fairly good precision ( $\pm 2\%$ ), and is capable of application up to at least a temperature of  $1200^{\circ}\text{K}$ . No absolute calorimetric measurements are necessary, which is a very desirable feature. Thus, the objective of this project is to use this new technique for obtaining data over a wide temperature range on pure gases and mixtures of propulsive interest.

### The O<sub>2</sub> - H<sub>2</sub>O System

The previous report (Ref. 1) summarized the experimental data obtained on the systems O<sub>2</sub>, 75% O<sub>2</sub> - 25% H<sub>2</sub>O, and 50% O<sub>2</sub> - 50% H<sub>2</sub>O over the temperature range 400-1100°K. Together with data on pure H<sub>2</sub>O (Ref. 2), these allowed a cross-plot of thermal conductivity vs. composition to be constructed at various temperatures. These are the plotted points labeled "EXPT" on Figure II-1. A set of theoretical curves (reproduced as curves "A" on Fig. II-1) were then obtained by ignoring the polar nature of H<sub>2</sub>O which were considerably at variance with the experimental data. This discrepancy has been examined during this quarter, and the theoretical treatment is recapitulated below.

A theory of the thermal conductivity of gas mixtures containing one or more polar components is not presently available in a satisfactory form for a real comparison of theory and experiment. A treatment of polyatomic and polar pure gases has recently been given by Mason and Monchick (Ref. 3) which includes effects due to relaxation and the resonant interchange of rotational energy. This work represented a distinct advance in the kinetic theory of gases and will no doubt be extended to mixtures in due course. Meanwhile, we shall have to be content with a less complete analysis for the present.

For non-polar gases, the mixture theory of Hirschfelder (Ref. 4) is available. Briefly, this theory assumes full equilibrium of all internal degrees of freedom with translation and the equality of the (self) diffusion coefficient for molecules in all internal energy states. The binary mixture relation is then

$$\lambda_m = \lambda_m^0 + (\lambda_1 - \lambda_1^0) [1 + (x_2 D_{11} / x_1 D_{12})]^{-1} + (\lambda_2 - \lambda_2^0) [1 + (x_1 D_{22} / x_2 D_{12})]^{-1} \quad (1)$$

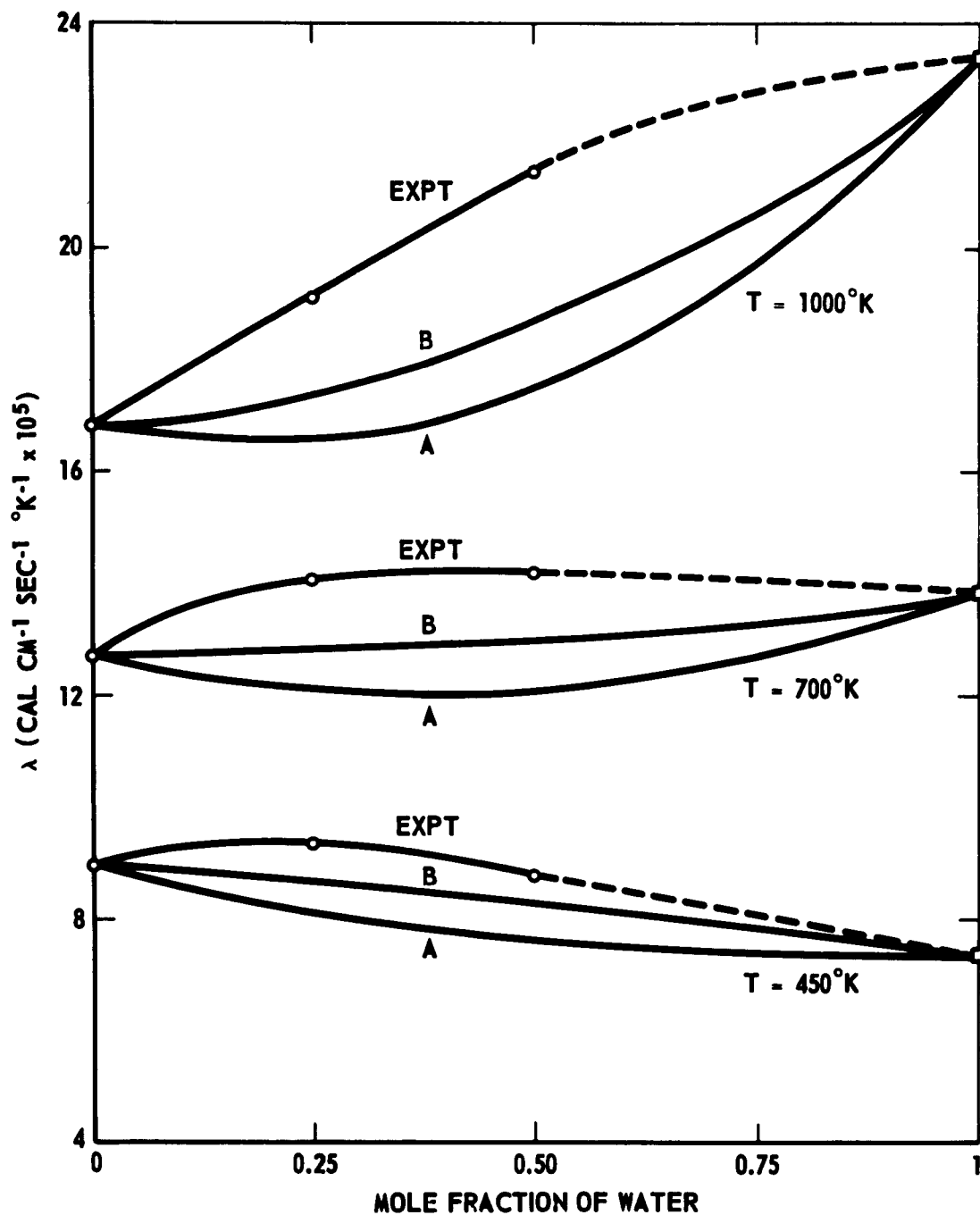


Fig. II-1 DEPENDENCE OF THE THERMAL CONDUCTIVITY OF  $O_2 - H_2O$  MIXTURES ON COMPOSITION AT VARIOUS TEMPERATURES

- : Experimental line source values.
- : Experimental values for pure  $H_2O$  taken from data of Ref. 2.
- Curves A: Theoretical results using Eq. (1) with experimental input data but neglecting polarity and rotational relaxation of  $H_2O$ .
- Curves B: Theoretical results using Eq. (1) with experimental input data and correcting  $H_2O$  for effect of resonant interchange and relaxation of rotational energy.

where  $\lambda_m^0$ ,  $\lambda_1^0$ , and  $\lambda_2^0$  are the translational thermal conductivities of the mixture and pure components 1 and 2,  $\lambda_1$  and  $\lambda_2$  are the pure component thermal conductivities,  $D_{11}$  and  $D_{12}$  are the self-diffusion coefficients,  $D_{12}$  is the binary diffusion coefficient, and  $x_1$  and  $x_2$  are mole fractions. For non-polar gases,  $\lambda_1^0$  and  $D_{11}$  can be related to the viscosity as was described in the earlier work on  $N_2 - CO_2$  (Ref. 5), so that these quantities can be obtained directly from experimental viscosity data when available. Use of Eq. 1 with all quantities either experimental ( $\lambda_1$ ,  $\lambda_2$ , and  $D_{12}$ ) or derived directly from experimental data by established kinetic theory relations ( $\lambda_1^0$ ,  $\lambda_2^0$ ,  $D_{11}$ ,  $D_{22}$ , and  $\lambda_m^0$ ) led to the curves labeled A in Figure II-1. These are uniformly lower than the experimental curves and do not predict the positive deviation from a linear mixture rule clearly shown by the experimental data. The discrepancy between curve A and experiment is as much as 20% for the 50-50 mixture at  $1000^\circ K$ . It is interesting that the behavior shown here is opposite to that found in the  $N_2 - CO_2$  case (Ref. 5), where the theoretical results were uniformly higher than experiment and showing positive deviations from linear mixing.

It is not unexpected, of course, to find a pronounced discrepancy between experiment and a theoretical treatment such as the foregoing which neglects the polarity of  $H_2O$ . As Mason and Monchick (Ref. 3) have recently shown, the main effect of polarity is to introduce the resonant interchange of rotational energy between two colliding molecules without any change in translational motion. This has the result of reducing the effective diffusion coefficient for transfer of internal (rotational) energy in a polar gas and thus reducing its thermal conductivity. Such a phenomenon should not influence the degree to which local equilibrium between internal and translational motions is attained. (This would not be the case for the rotational relaxation effect in polyatomic molecules also treated by Mason and Monchick, which by definition is a non-equilibrium phenomenon.)

Thus it would seem roughly plausible at least, that the basic mixture relation (1) could still be used with a polar component present providing the correct value of  $D_{11}$  (letting 1 represent  $H_2O$ ) is used. In the derivation of Eq. 1,  $D_{11}$  really enters as the effective self-diffusion coefficient for internal energy, which is only equal to the ordinary self-diffusion coefficient when no complicating effects such as polarity are present. As outlined in Ref. 3, the ordinary  $D_{11}$  computed from viscosity should be corrected for resonant interchange by the factor  $(1 + Z'/Z_0)^{-1}$ , where  $Z'/Z_0$  is a fairly complex function of temperature, dipole moment, and the moments of inertia (among other things). Thus we have

$$(D_{11})_{\text{polar}} = D_{11} (1 + Z'/Z_0)^{-1} \quad (2)$$

Similarly, the translational contribution to the thermal conductivity,  $\lambda_1^0$ , needs to be corrected for the resonance effect. Again following Mason and Monchick, this can be done by making use of the factor  $f_{\text{tr}}$  which is a function of  $Z'/Z_0$  as well as the rotational relaxation time. The latter is introduced by way of the rotational relaxation collision number  $Z_{\text{rot}}$  which was taken equal to 4 and independent of temperature. The factor  $f_{\text{tr}}$  thus includes both the polarity effect (resonant collisions) and that of rotational relaxation. In this way, from the value of  $\lambda_1^0$ , derived from viscosity we get

$$(\lambda_1^0)_{\text{polar}} = f_{\text{tr}} \lambda_1^0 \quad (3)$$

When both  $(D_{11})_{\text{polar}}$  and  $(\lambda_1^0)_{\text{polar}}$  were used in Eq. 1 instead of the uncorrected values, the curves labeled B in Figure II-1 were obtained. It is clear that some improvement compared to the experimental curves is afforded by this approximate procedure, although there is still an appreciable discrepancy. All that can be said at present is that inclusion of resonant interchange and rotational

relaxation is a step in the right direction, and that further improvement must await a more rigorous extension of the theory to mixtures. Presumably this will yield a better version of Eq. 1.

References

- 1) Task R Quarterly Progress Report No. 14, The Johns Hopkins University, Applied Physics Laboratory Report No. TG-331-14.
- 2) N. B. Varagaftik and O. N. Oleschuk, Izvest. VII 15, #6, 7 (1946).
- 3) E. A. Mason and L. Monchick, J. Chem. Phys. 36, 1622 (1962).
- 4) J. O. Hirschfelder, Sixth Symposium on Combustion, Reinhold, New York (1957) p. 351.
- 5) A. A. Westenberg and N. de Haas, Phys. Fluids 5, 266 (1962).

### III. ROCKET NOZZLE FLUID DYNAMICS

(F. K. Hill and H. J. Unger)

#### Objective

Experimental data have been collected on which to base an understanding of the fluid dynamic processes which take place in rocket nozzles. Solid propellants generate a high-temperature gas that forms a complex fluid system during its passage from the combustion chamber to the nozzle and rapidly expands into supersonic flow. Due to the fact that the gas is composed of a mixture of substances, the fluid properties are difficult to predict precisely. For this reason, it has been considered worth while to acquire experimental data on chemical reaction rates, the concentration of species, boundary layer characteristics, surface reaction and heat transfer rates of the gas.

Techniques developed for use in supersonic and hypersonic wind tunnels have been used to gather experimental boundary layer data in the supersonic section of the rocket nozzle. Detailed boundary layer properties may be used to accurately compute skin friction and heat transfer coefficients as functions of non-dimensional parameters such as Reynolds number, Mach number, etc. These coefficients provide the fundamental data for the design and fabrication of improved nozzles. The environmental conditions at the throat of the nozzle are so severe that one cannot employ conventional fluid dynamic measuring equipment. For this reason, one searches for other techniques for the determination of heat transfer properties.

Present experiments with the rocket tunnel have been conducted with a double-base propellant, ARP, manufactured by the Allegany Ballistics Laboratory. During combustion at 1100 psig and 2500°K, carbon dioxide, carbon monoxide, water vapor, hydrogen, and nitrogen are generated as the principal components of the gas. The

first three of these components are active infrared absorbers in the spectral region, 4 to  $6.5\mu$ . In order to determine the composition of the gas mixture as it passes through the nozzle, an infrared absorption technique has been adapted for observing the flow at various stations. This system avoids any interference with the flow and is limited only by the gas sensitivity to the radiation that is transmitted through the flow. Absorption measurements of the gases are undertaken for the purpose of determining their concentration as well as their temperature. The infrared technique has been developed to utilize not only absorption, but emission properties as well. This method of observation is expected to be used on propellants with combustion temperatures in the area of  $3500^{\circ}$  to  $4000^{\circ}$ K. The species evolved in the combustion of these higher energy propellants are more numerous, more complicated, and include appreciable fractions of solid particles and free radicals.

It is hoped that the techniques developed in these studies will be applicable to a wide gamut of propellants whose efficient utilization will depend to a large extent on a better comprehension of the physical and chemical processes taking place in the nozzle.

#### Review of Experimental Results

An experimental technique has been worked out for using a narrow cross-section of the rocket tunnel as an absorption cell or as a source of emission from the gas. Slits in the tunnel wall covered by side tubes containing infrared transmission windows comprise the cell. The windows are protected from hot gas by flushing toward the tunnel slits with nitrogen. This system has been very satisfactory as far as protecting the windows is concerned. The same  $\text{CaF}_2$  windows are in use after many tests without acquiring a single scratch or chip.

Absorption spectra in the 4 to  $6.5\mu$  region have been observed with a fast scanning spectrometer at various conveniently located stations along the tunnel, starting with the four-inch section

in the fully expanded region where the pressure and temperature were approximately 1.5 psia and 600°K. Successive tests were conducted at the 3.5-inch, 3.00-inch, 2.33-inch, 1.86-inch, 1.38-inch, 1.06-inch, and 0.803-inch stations. At the last station the conditions were 167 psig and 1700°K. The main objective of this series of tests was to establish the experimental technique of determining the composition of the gas at any station along the tunnel without sampling, and also to make a spectroscopic determination of the temperature. Various mechanical and electrical problems (ambient sound level in the test area was 150 db) had to be solved to attain a signal to noise ratio of 100 during tunnel operation.

The spectrometer was originally designed to make absorption and emission observations by using a single chopper at the spectrometer entrance slit. This method is consistent as long as the calibration is done in the same manner as the observations. Difficulty is encountered when the spectral emissivity of the gas approaches that of the source. Figure III-1 shows the absorption plus the emission at the 0.803-inch station where the temperature is of the order of 1700°K. The emission exceeds the absorption where the deflection went off-scale in the region around 4.5 $\mu$ . The absorption band of CO<sub>2</sub> at 4.25 $\mu$  is that of the gas at relatively low temperature, near ambient. The only apparent explanation of this observation is that gas from the tunnel is escaping into the side tubes, cooling down and increasing the effective cell length. A confirmation of this difficulty is shown in Figure III-2, which is an emission spectrogram taken at the 0.803-inch station. One observes emission from CO<sub>2</sub>, CO, and H<sub>2</sub>O with narrow band absorption superimposed. Figure III-3 was taken with the chopper at the source and observation at the 1.38-inch station. This is absorption only and shows the band broadening due to high temperature. The P-branch of the CO<sub>2</sub> band extends into the R-branch of the CO band. The effect of cold gas in the side tubes is evident in the P-branch of the CO band which causes two absorption maxima. It appears that



Fig. III-1 ABSORPTION SPECTROGRAM AT THE 0.803 STATION WHERE THE PRESSURE WAS 167 PSIA AND THE TEMPERATURE 1700°K

Light from the Nernst glower was chopped at the spectrometer slit so the apparent absorption is really absorption minus emission from the gas. The 4.25  $\mu$   $\text{CO}_2$  band is narrow as that of a gas at ambient temperature. This indicates the presence of cold gas in the side tubes that support the windows.



Fig. III-2 THE EMISSION-ABSORPTION SPECTRUM AT THE SAME TUNNEL STATION USED IN FIG. III-1

The same 4.25 $\mu$  CO<sub>2</sub> absorption band is present indicating there was cold gas in the side tube. The Nernst glower source was off.

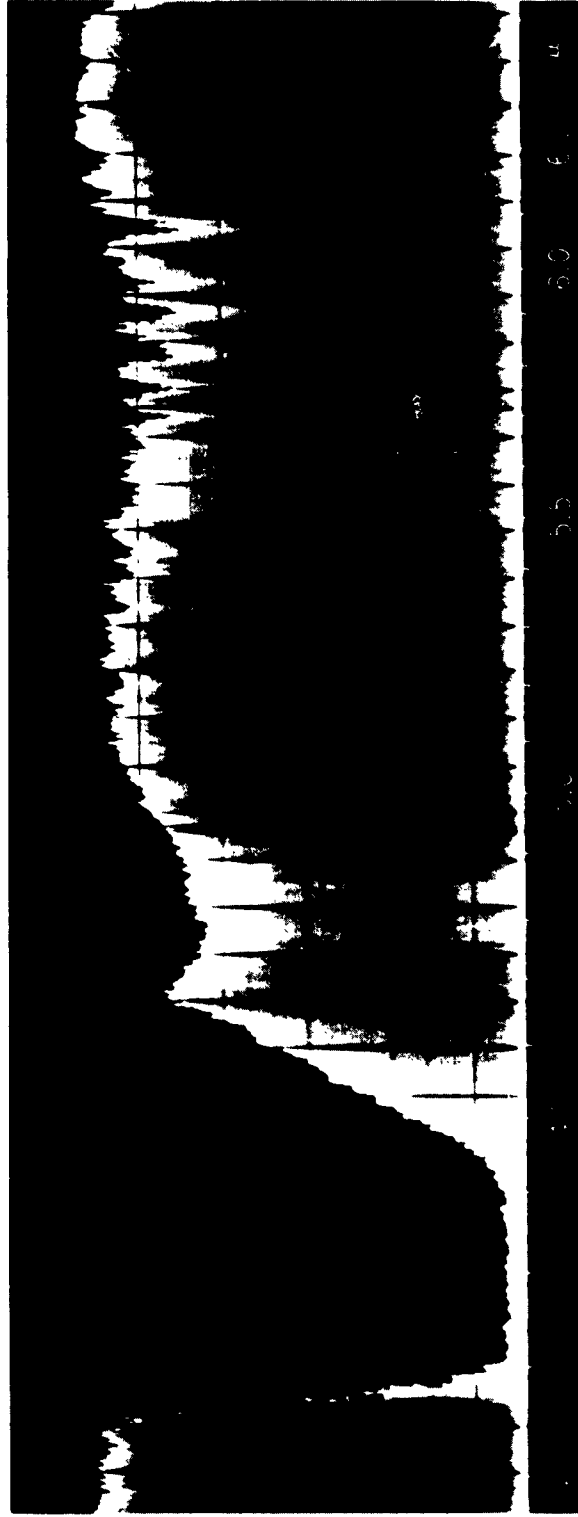


FIG. III-3 THE TRUE ABSORPTION SPECTRUM OF THE HOT TUNNEL GAS  
AT THE 1.38-INCH STATION

The temperature broadening of the bands is very evident. The R-branch of the CO band overlaps the P-branch of the CO<sub>2</sub> band. Absorption by cold gas in the side tubes is evident by the double dip in the P-branch of the CO band. Nernst glower source is on and the light chopper is between the source and the tunnel.

further flushing tests are necessary to establish the correct flushing pressure to prevent gas from the tunnel from entering the side tubes. Elimination of the absorption spectrum superimposed on the emission spectrum is probably the most sensitive test for the correct flushing pressure.

Figure III-3 of the previous report, No. 14, is reproduced here as Figure III-4. These data were obtained from a free jet and consist of absorption and emission curves observed with the light chopper at the spectrometer entrance slit. The pressure and cell length were kept constant in each case and only the temperature varied. If we let

$A_{\lambda}$  = the maximum spectral absorption in the cell of the light from the source,

$E_{\lambda}$  = the maximum spectral emission from the hot gas in the cell,

$A_{s\lambda}$  = the maximum spectral self-absorption of the emission from the hot gas,

then one curve is  $A_{\lambda} - E_{\lambda} + A_{s\lambda}$  and the other  $E_{\lambda} - A_{s\lambda}$ . The sum of these curves at any temperature is the spectral absorption of light from the source.  $(A_{\lambda} - E_{\lambda} + A_{s\lambda}) + (E_{\lambda} - A_{s\lambda}) = A_{\lambda}$ . This is another proof that the maximum spectral absorption of  $CO_2$  is independent of temperature.

All of the above evidence leads to the conclusion that the window flushing system must be re-examined for use in high pressure flow. The difficulty of not being able to vary the path length or the partial pressure of the gas in the tunnel absorption cell is a serious limitation to good quantitative absorption measurements. Normally, one uses the maximum absorption in an unresolved branch of the band as the absorption index. When this is not possible due to too much absorption, the only alternatives are to choose a weaker band or select a wavelength on the side of the branch at a favorable absorption value as an index. This would be a valid method as long as the temperature of the gas did not change.

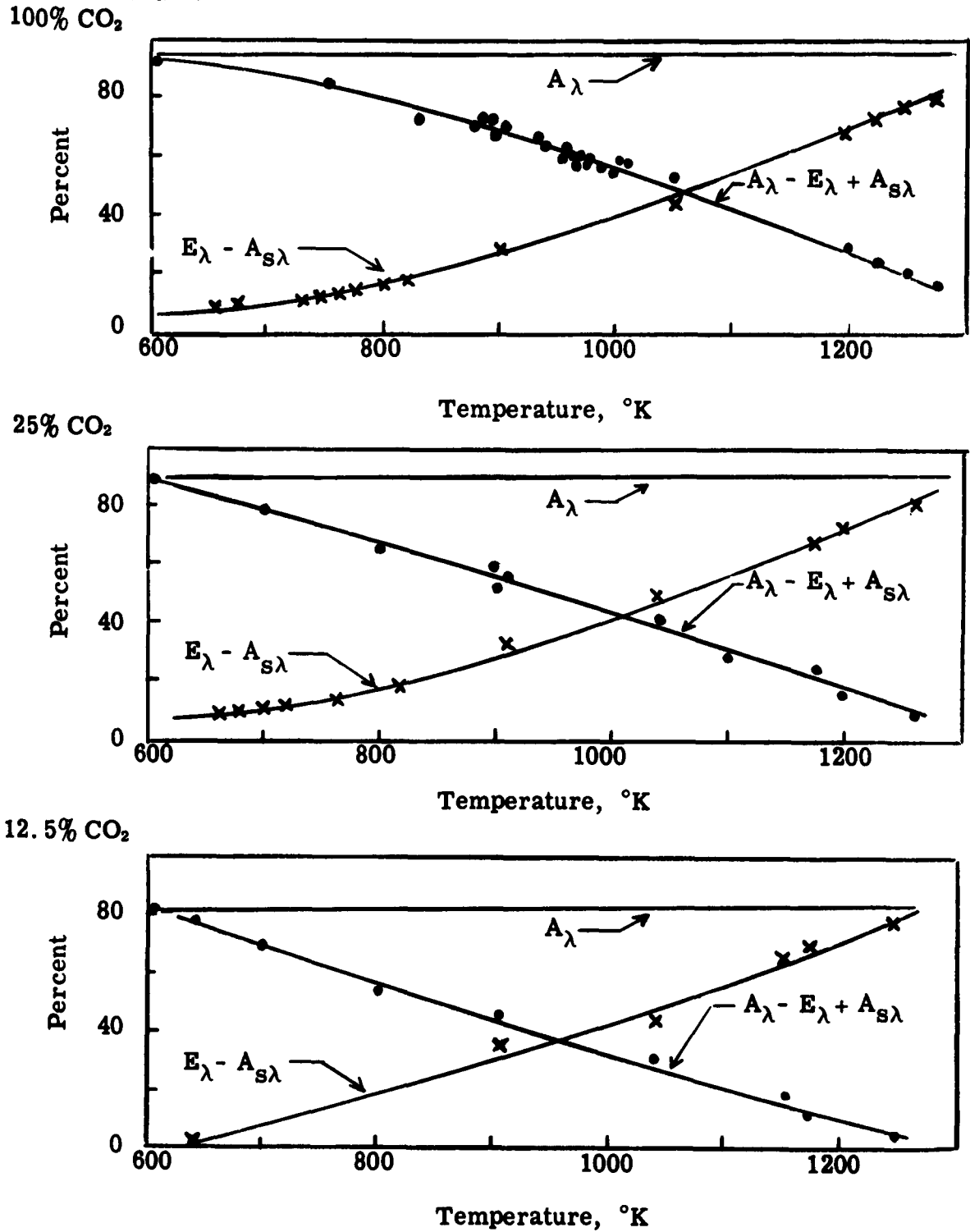


Fig. III-4 CO<sub>2</sub> Emission and Absorption at 4.25 μ as a Function of Temperature  
 Path Length = 1.2 in., Pressure 1 Atmosphere

These curves show that the absorption of CO<sub>2</sub> is independent of temperature up to 1300 °K.

Conclusions

At the higher temperature and pressure stations in the nozzle - i.e., nearer the throat - the present window flushing technique is inadequate to confine the tunnel gas. Further tests with variable flushing pressure during the run should be made while observing the emission spectra for evidence of absorption. This should be a sensitive means of determining the correct flushing pressure.

In cases where the maximum absorption approaches extinction, it will be necessary to choose a wavelength index on the side of the absorption band instead of the position of maximum absorption.

#### IV. MOLECULAR BEAM CHEMICAL KINETIC STUDIES

(R. M. Fristrom and C. Grunfelder)

##### Objective

Reactions between species in the form of beams of well-defined energies offer an attractive way to study chemical kinetics of elementary reactions. By analysis of the scattered product distribution from two such interacting beams, it is possible to derive data on the activation energy and steric factor of the reaction. One of the main barriers to the practical application of the beam approach has been lack of a satisfactory method of creating beams of sufficient intensity and low enough energy (for chemical reactions) for convenient use with common detection methods. This project aims to attack this problem by exploiting a new approach being developed at APL. This involves the creation of an aerodynamic (supersonic) beam by progressive removal of the boundary layer through the porous walls of a nozzle. This technique should accomplish the same thing as a supersonic nozzle beam but with much simpler pumping requirements.

##### Advantages and Disadvantages of the Beam Technique for Studying Chemical Kinetics

Some of the outstanding advantages of the beam approach to kinetic studies are:

1. Since the reactions only involve a single collision between known species, it is possible to establish unambiguously what reaction is being studied without complications from subsequent reactions or back reactions.
2. The problem of mixing and premixing reactants does not exist.

3. The effective temperature of the reaction can be varied over a wide range independently of the properties such as vapor pressure of the material. This allows reactions between otherwise incompatible species to be studied. The effective collision velocity of a molecule is some two to five times the velocity corresponding to the temperature of the precursor gas, and in a reaction study this velocity can be added to that of the reacting species by opposing the two beams; thus a reaction can be studied at some five to ten times the effective temperature possible by other techniques.

4. There are no complications associated with wall effects.

5. By analyzing the detailed scattering pattern, both with respect to direction and velocity, it should be possible to examine the detailed mechanics of the collision. From this, data on activation energy and steric factor can be derived. In some cases, the mass spectrometer may allow the identification of the excited state from its mass spectrum and appearance potential. Ultimately, even more detailed determinations could be made, but these refinements are far in the future.

The main disadvantages are:

1. The beam apparatus and associated equipment is complex and difficult to operate.

2. The interpretation of beam kinetic results in terms of more conventional concepts (rate constants, etc) is not always straight forward.

#### Proposed Experiment

It is proposed to scatter two high intensity beams and measure the angular and velocity distribution of the scattered molecules using a time of flight mass spectrometer as a detector. This will be done by modulating the reacting beams with mechanical chopping of  $10^{-4}$  sec duration at a convenient repetition rate (10-100 cps). The

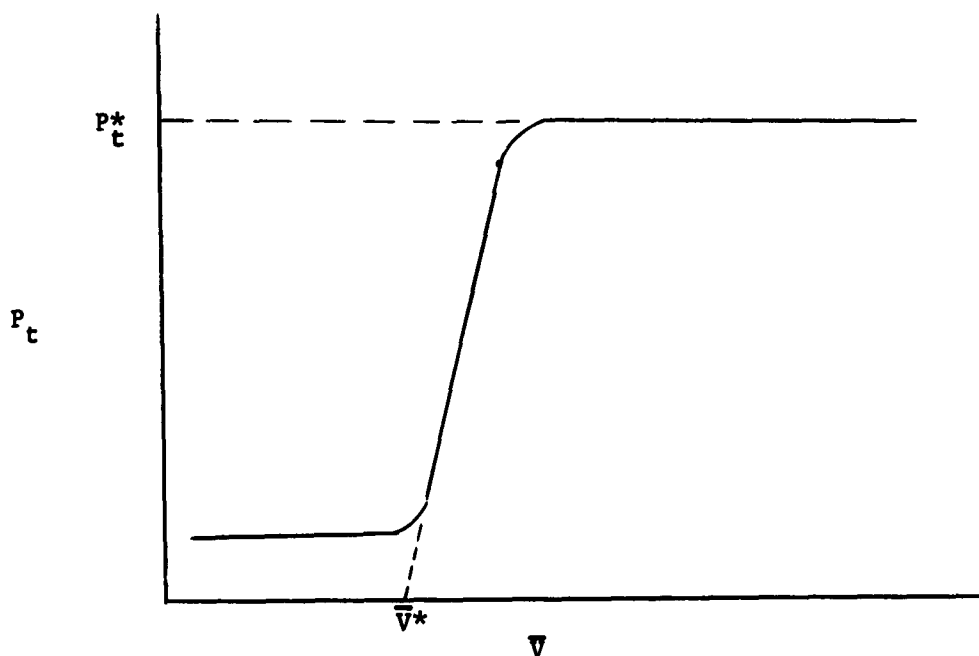
detecting mass spectrometer is located at a fixed distance and position. It accepts a known solid angle of the scattered molecules. Thus, the output will be the arrival time of the scattered molecules in a known solid angle. This is the inverse of the velocity distribution and provides information on both the angular distribution of reacting species and their momentum. The signal will be repeated at the modulation frequency giving an increase in sensitivity through averaging techniques.

The complete interpretation of crossed molecular beam chemical kinetic experiments is a complex exercise in molecular mechanics (Ref. 1). Our information will be somewhat more detailed than the usual experiments since we hope to provide velocity (i.e. molecular momentum) data as well as the angular distribution of products. This additional information should allow some simplifications of the interpretation. These questions are being considered, but it is hardly an immediate problem since no crossed beam data are expected before the end of the year.

The first order interpretation of crossed beam information seems straightforward and is instructive since it clearly shows the connection between classical chemical kinetics and molecular beam experiments. If one considers the reaction in crossed molecular beams of two species of known velocity colliding at a known angle  $\alpha$ , the quantity which is measured is  $P(\theta)$ , the ratio of scattered products to scattered reactants in a small solid angle,  $\theta$ . This is the ratio of the number of reacting collisions to the total number of collisions. This quantity integrated over all angles  $\theta$  gives the total scattering ratio  $P_t$ . This quantity is determined for a range of relative beam velocities,

$$\bar{v} = \sqrt{v_1^2 + v_2^2 - \frac{1}{2}v_1v_2 \cos \alpha} \quad (1)$$

and the results plotted. The form would be expected to be as in the following sketch:



$P_t$  would be essentially zero until a critical velocity  $\bar{v}^*$  is reached. At this point the collision efficiency rapidly rises to a plateau value,  $P_t^*$ . The  $\bar{v}^*$  corresponds to the classical activation energy

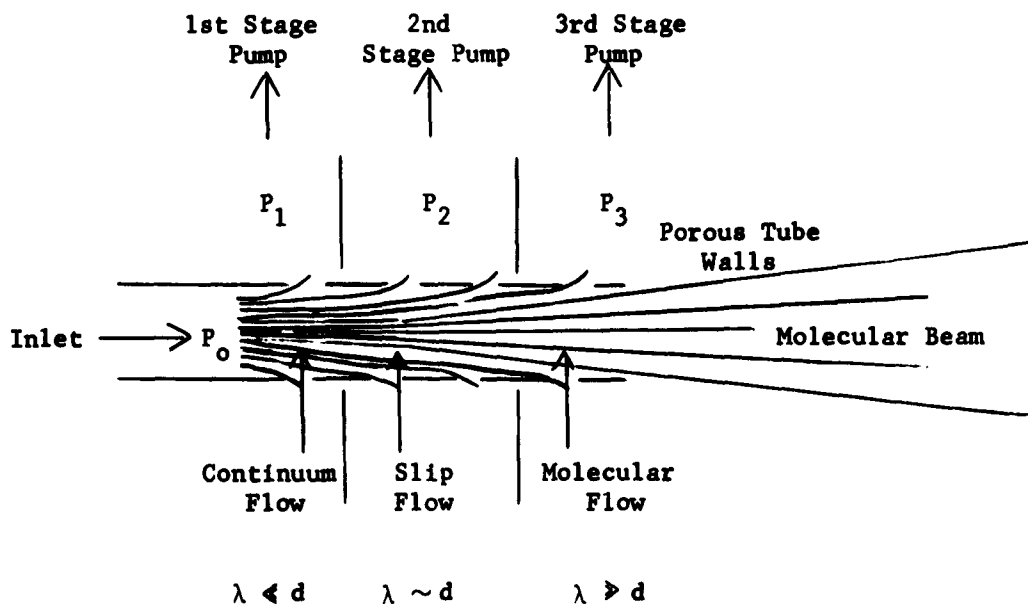
$$E = \frac{1}{2}m(\bar{v}^*)^2 \quad (2)$$

while  $P_t^*$  corresponds to the steric factor. If the geometry and strength of the colliding beams are well known, one can derive the classical scattering cross section from the ratio of total scattered flux to total beam flux. The shape of the region of steep rise contains information concerning the potential surfaces of interaction of the reacting molecules, but this information may be easier to extract from the detailed angular and velocity studies.

Beam Design

The critical component for these studies is the molecular beam. It must have sufficient intensity so that both elastic and inelastic scattered components can be detected. For chemical reaction experiments, the relative velocity of the two beams must be sufficient for reaction to occur, and be of known (preferably narrow) velocity distribution.

The beam intensity required to give a reasonable scattered signal with 50 cm separation is of the order of  $10^{17}$  molecules  $\text{cm}^{-2} \text{sec}^{-1}$ . Intensities of this order have been obtained (Ref. 2) using a convergent nozzle and free space expansion, but the pumping speeds required are extremely high ( $10^4$  L/sec). It is expected that these requirements can be reduced substantially by use of the porous nozzle technique. Referring to the sketch below,



a nozzle of rectangular cross-section with two porous walls has been constructed. This allows the boundary layer to be pumped off in stages, and most of the material can be removed in the early stages at relatively high pressure. A nozzle of minimum size can thus be used, which reduces overall pumping requirements. The Mach number is a measure of the ratio of the directed velocity to the random (thermal) velocity, and since  $M \sim 10$  or higher are feasible, rather narrow velocity cuts are possible. Estimates of the performance of such a nozzle can be made by assuming continuum flow without boundary layer until the density drops to the point where the nozzle diameter is less than a mean free path. The flow is then assumed collision-free beyond this point. Upper limits of performance estimated in this way indicate fluxes of the order of  $10^{19}$  molecules  $\text{cm}^{-2} \text{sec}^{-1}$  for a system a few millimeters wide.

Since boundary layer pumping removes material which has made wall collisions, porous walled nozzles may also be useful as sampling probes for free radicals and other species which are destroyed by wall reactions. In the porous nozzle, material adjacent to the wall is removed leaving a core which has made no (or very few) collisions with the walls.

#### Preliminary Trials

Two preliminary experiments have been undertaken to test the porous walled nozzle concept. A porous electroformed nickel nozzle was surrounded by a dry ice cooling tube. This tube was fed by a furnace containing metallic sodium and the system scavenged by a small oil diffusion pump. The beam was visualized by cross illumination from a sodium resonance lamp. A sharp, well-formed beam was produced, which was scattered by an effusive beam of methyl iodide. As the intensity of the  $\text{CH}_3\text{I}$  beam was increased, the sodium beam faded until it became invisible. Analysis of the gases taken by the scavenger pump showed traces of ethane in a concentration corresponding to 1 percent conversion of the methyl iodide. This was at least partially due to a beam reaction since,

when the same flux of methyl iodide was introduced into the chamber by another inlet, the concentration of ethane in the pumped gases dropped to half a percent. No quantitative significance should be attached to the results, however. Background fog of scattered light indicated that the freezeout efficiency of glass surfaces is not high, as has been observed by other experimenters (Ref. 3).

A second test of the nozzle technique was made using the Bendix Time of Flight Spectrometer as a detector. Using inlet pressures of one mm of argon, beam intensities were obtained which were estimated to be greater than  $10^{14}$  molecules per sec per  $\text{cm}^2$ . This flux gave a spectrometer a signal 10 times higher than the limit of linearity. The acceptor pump in the spectrometer proved to be the limiting factor. Since 1 mm was the lowest pressure for continuum operation of the nozzle and there is a strong increase in flux with operating pressure in this range (Ref. 1), it is felt that with improved pumping and repetitive operation, the required beam intensities will be attained.

#### References

- 1) S. Datz, D. Herschback and E. A. Taylor, "Collision Mechanism Crossed Maxwellian Molecular Beams," *J. Chem. Phys.* 35, 1549 (1961).
- 2) G. R. Isaak, "An Atomic Beam Spectro Photometer," *Nature* 189, 373 (1961).
- 3) J. Deckers and J. B. Fenn, "A High Intensity Molecular Beam Apparatus," Project SQUID Tech. Report PR103-P, Princeton Univ., June 1962.

Initial distribution of this document has been made in accordance with a list on file in the Technical Reports Group of The Johns Hopkins University, Applied Physics Laboratory.